Study of Hitting Time and Probability for Random Walks in One and Two Dimensions

Research Result Report
College Student Research Scholarship
National Science and Technology Council

Yung-Hsuan Chang

March 2026

Erratum (June 2026). Corrected the identification of $E(0,0)$—it is the centroidal value of the Prandtl stress function, not the torsional rigidity; a subscript typo in the generator's definition, $S_{t+1} \to S_{n+1}$, was also fixed. Numerical results and conclusions are unaffected.

一維與二維隨機漫步之擊中時間與機率研究

國家科學及技術委員會大專學生研究計畫成果報告

張永璿

2026 年 3 月

勘誤（**2026** 年 **6** 月）。更正 $E(0,0)$ 之物理意義——其為普朗特應力函數（Prandtl stress function）在形心處之值，而非扭轉剛度（torsional rigidity）；另修正生成元（generator）定義中的下標誤植，$S_{t+1} \to S_{n+1}$。數值結果與結論均不受影響。

摘要

本研究深入探討簡單隨機漫步（simple random walk）在不同維度與參數設定下的擊中時間分布（hitting time distribution）與期望擊中時間（expected hitting time）。在簡單對稱隨機行走的既有研究基礎上，我們進一步分析了有偏（biased）簡單隨機漫步的行為，推導出非對稱機率 $p \neq q$ 下的擊中時間分布與期望擊中時間解析解，展示了在雙邊界中偏移帶來的漂移（drift）如何使期望擊中時間的尺度律由二次成長變為漸近線性（asymptotically linear）。針對二維情形，我們證明了特定線性邊界問題可透過坐標變換降維至一維模型求解。最後，我們比較了菱形、圓形與正方形等幾何邊界對期望擊中時間的影響，數值結果顯示期望擊中時間皆與特徵長度的平方（N^2）成正比。具體而言，數值斜率分別收斂至 ≈ 0.589（菱形）、≈ 1.0（圓形）與 ≈ 1.179（正方形）。我們證實這些常數對應於彈性力學中不同截面之扭轉應力函數（torsion stress function）在形心處的最大值，並探討了面積與形狀效率之間的關聯，最後透過數值模擬驗證了旋轉不變性的物理特性。

關鍵字：簡單隨機漫步、擊中時間分布、期望擊中時間、扭轉應力函數

Abstract

This report provides a comprehensive analysis of hitting time distributions and expected hitting times for simple random walks across different dimensions and parameter regimes. Expanding upon the simple symmetric case, we incorporate biased simple random walks ($p \neq q$) into our framework, deriving analytical solutions for hitting time distributions and expected hitting times. We demonstrate that introducing bias, which induces a drift, alters the scaling of expected hitting time in a two-boundary condition from quadratic to asymptotically linear. In the two-dimensional context, we show that certain linear boundary problems can be reduced to one-dimensional models via coordinate transformation, and we investigate the impact, on expected hitting time, of domain geometry by comparing diamond, circular, and square boundaries. Our numerical simulations confirm that the expected hitting time scales as $C \cdot N^2$, where C is a shape-dependent constant. Specifically, our numerical estimates for C align with theoretical predictions: ≈ 0.589 for the diamond, ≈ 1.0 for the circle, and ≈ 1.179 for the square. We provide a theoretical verification of these constants by linking them to the centroidal (maximum) value of the torsion stress function of corresponding cross-sections in continuum mechanics. Furthermore, we analyze the relationship between domain area and hitting time efficiency, and empirically validate the rotation invariance of the underlying diffusion process through high-density numerical sampling.

Keywords: Simple Random Walk, Hitting Time Distribution, Expected Hitting Time, Torsion Stress Function

Contents

List of Figures **IV**

1 Introduction **1**

2 Research Objectives **1**

3 One-Dimensional Random Walk **1**
3.1 Hitting Time Distributions 2
3.1.1 Single Boundary at N 2
3.1.2 Two Boundaries at $-N$ and N 2
3.2 Expected Hitting Time 3
3.2.1 Single Boundary at N 3
3.2.2 Two Boundaries at $-N$ and N 3

4 Two-Dimensional Random Walk: Reductions for Unbounded Boundaries **4**
4.1 Line Boundary ($x + y = N$) 4
4.2 Strip Boundary ($|x + y| = N$) 4

5 Two-Dimensional Random Walk: Comparison of Expected Hitting Times for Bounded Boundaries **5**
5.1 Expected Hitting Time and the Discrete Poisson Equation 5
5.1.1 Explicit Solution for $N = 2$, General (Diamond Domain) 5
5.1.2 Explicit Solution for $N = 3$, Unbiased (Diamond Domain) 6
5.2 Asymptotic Scaling and Data Collapse 7
5.3 Numerical Comparison of Domain Geometries, Unbiased 7
5.3.1 Diamond Domain (L^1-Ball) 9
5.3.2 Circular Domain (L^2-Ball) 9
5.3.3 Square Domain (L^∞-Ball) 10
5.4 Difficulties Encountered and Solutions 10
5.5 Bonus: Universal Scaling in Higher Dimensions for the Circular Domain . . 11

6 Conclusion **12**

Acknowledgments **12**

Appendix A: Derivation of the Expected Hitting Time for One Boundary **12**

Appendix B: Derivation of the Expected Hitting Time for Two Boundaries **14**

References **15**

List of Figures

1 Asymptotic universality of the hitting time distribution. 7
2 The comparison of hitting time distributions between random walk and planar Brownian motion. 8
3 Comparison of the expected hitting time scaling across three different geometries. 8
4 Comparison of the expected hitting time scaling across four different geometries. 10

1 Introduction

The random walk is a ubiquitous model in probability theory, serving as the discrete foundation for continuous stochastic processes. Under appropriate scaling limits, the random walk converges to Brownian motion, a result formalized by the functional central limit theorem (Donsker's theorem). This correspondence allows the random walk to act as a powerful analytical tool for investigating diffusions, stochastic differential equations, and their associated partial differential equations, particularly through the connection between the discrete generator and the continuous Laplacian operator. While the recurrence of simple (nearest-neighbor) symmetric random walks in low-dimensional lattices is a well-established classical result [1, pp. 35–53, 2, p. 75], the quantitative characteristics of the expected hitting time of a boundary remain a subject of significant interest, revealing intricate dependencies on the domain geometry.

This report extends the existing literature by introducing asymmetry into the random walk dynamics. We analyze the biased simple random walk, characterized by unequal transition probabilities ($p \neq q$), to systematically study the interplay between fluctuations and directional bias within a discrete lattice, and to further investigate the asymptotic behavior of the expected hitting time. This formulation provides a rigorous discrete analog to drift-diffusion phenomena. Furthermore, we expand our investigation to two-dimensional domains, specifically examining how boundary geometry (diamond, circle, square) influences the asymptotic behavior of the exit time. This approach bridges the gap between discrete probabilistic models and their continuum limit solutions across varying geometries.

2 Research Objectives

The primary goals of this research are structured to progress from fundamental one-dimensional cases to complex two-dimensional geometries.

1. **One-Dimensional Random Walk**: Derive the hitting time distribution and expected hitting time for simple random walks on an interval.
2. **Two-Dimensional Random Walk**:
   (a) Reductions for Unbounded Boundaries: Analyze random walks bounded by lines ($x+y = N$) and strips ($|x+y| = N$) by reducing them to one-dimensional equivalent problems.
   (b) Comparison for Bounded Boundaries: Analyze and compare the expected hitting times for diamond (L^1-ball), circular (L^2-ball), and square (L^∞-ball) domains to identify the shape-dependent scaling constants.

3 One-Dimensional Random Walk

Consider a random walk $(S_n)_n$ on $\mathbb{Z}$ starting at $S_0 = 0$. Let p be the probability of a step $+1$ and $q = 1 - p$ for a step -1. We consider two cases: boundary at $N \in \mathbb{N}$ and

⋆ *Note*: The "probability" aspect of the proposal is specifically explored here through the lens of "hitting time distributions" rather than asymptotic hitting probabilities; also, we focused on simple random walks. To be more precise, the title would be more ideal as "Study of Hitting Time for Simple Random Walks in One and Two Dimensions".

boundaries at $-N$ and N.

We will use τ_N to indicate the first hitting time of the boundary. In the following context, "first" will be omitted. For the single boundary case, we define

$$\tau_N \coloneqq \min\{n \in \mathbb{N} : S_n = N\}. \tag{3.0.1}$$

For the two boundary case, we use the same notation but different stopping conditions,

$$\tau_N \coloneqq \min\{n \in \mathbb{N} : S_n = N \text{ or } S_n = -N\}. \tag{3.0.2}$$

3.1 Hitting Time Distributions

In this section, we derive the probability that the walk hits the boundary for the first time at step n, namely $f_{\tau_N}(n) = \mathbb{P}(\tau_N = n)$.

3.1.1 Single Boundary at N

Note once again that the definition of τ_N in (3.0.1) implies that the walk is not stopped if it hits $-N$. Going from 0 to N is in fact going from 0 to 1 and then from 1 to N. Also, by the translation invariance of the walk, we know that the probability of hitting 1 from 0 is the same as the probability of hitting N from $N-1$. Therefore, it follows immediately that

$$G_{\tau_N}(x) = (G_{\tau_1}(x))^N,$$

where $G_{\tau_N}(x)$ is the generating function of τ_N, i.e.,

$$G_{\tau_N}(x) = \sum_{n=0}^{\infty} f_{\tau_N}(n) x^n.$$

By [3, pp. 6–9], it follows that

$$G_{\tau_N}(x) = \left(\frac{1 - \sqrt{1 - 4pqx^2}}{2qx}\right)^N. \tag{3.1.1}$$

By expanding the generating function, we can derive the hitting time distribution,

$$f_{\tau_N}(2k - N) = p^k \cdot q^{k-N} \cdot \frac{N}{2k - N} \cdot \binom{2k - N}{k}.$$

Equivalently, in terms of $n = 2k - N$,

$$f_{\tau_N}(n) = p^{\frac{n+N}{2}} \cdot q^{\frac{n-N}{2}} \cdot \frac{N}{n} \cdot \binom{n}{\frac{n+N}{2}}, \tag{3.1.2}$$

for $n \geq N$ and $n \equiv N \mod 2$; zero otherwise.

3.1.2 Two Boundaries at $-N$ and N

Note once again that the definition of τ_N in (3.0.2) implies that the walk will stop if it hits $-N$.

This formulation corresponds to the classical gambler's ruin problem, where both ruin and reaching the target wealth are treated as identical absorbing states. Thus, we consider

this as a gambler's ruin problem with initial wealth N, target wealth $2N$, and probability of winning p.

Applying the hitting time distribution in the gambler's ruin problem [4], the probability of hitting 0 before $2N$ starting from N at step n is given by

$$p(n;p,q) \coloneqq 2^n p^{\frac{n-N}{2}} q^{\frac{n+N}{2}} \frac{1}{2N} \sum_{k=1}^{2N-1} \cos^{n-1}\left(\frac{k\pi}{2N}\right) \sin\left(\frac{k\pi}{2N}\right) \sin\left(\frac{k\pi}{2}\right). \tag{3.1.3}$$

Thus, our desired hitting time distribution is the combination of the probability of hitting 0 before $2N$ and the probability of hitting $2N$ before 0, which is given by

$$f_{\tau_N}(n) = p(n;p,q) + p(n;q,p) \tag{3.1.4}$$

for $n \geq N$ and $n \equiv N \mod 2$; zero otherwise. The choice between $\{0, 2N\}$ and $\{-N, N\}$ does not affect the hitting time distribution due to the translation invariance of the walk.

The solution in (3.1.3) can be physically interpreted through the reflection principle. To satisfy the absorbing boundary conditions at both ends, one effectively superimposes the contributions from an infinite sequence of "mirror" sources located at $\{\ldots, -5N, -3N, -N, N, 3N, 5N, \ldots\}$. Mathematically, the resulting trigonometric summation represents the Fourier series expansion of the probability distribution. The terms in the sum correspond to the eigenfunctions of the discrete Laplacian operator on the finite interval, providing a discrete counterpart to the separation of variables method used in solving the heat equation.

3.2 Expected Hitting Time

3.2.1 Single Boundary at N

Note once again that the definition of τ_N in (3.0.1) implies that the walk is not stopped if it hits $-N$.

Recall that we have a generating function in (3.1.1). Since the radius of convergence is not guaranteed to strictly exceed 1, we obtain the defective mean by taking the left limit of the derivative of $G_{\tau_N}(x)$ as $x \to 1^-$ [3, pp. 9–10]. By the chain rule, we have

$$\frac{\mathrm{d}G_{\tau_N}}{\mathrm{d}x}(x) = N \cdot (G_{\tau_1}(x))^{N-1} \cdot \frac{\mathrm{d}G_{\tau_1}}{\mathrm{d}x}(x).$$

Taking the limit $x \to 1^-$ (detailed in Appendix A) yields

$$\mathbb{E}(\tau_N) = \lim_{x \to 1^-} \frac{\mathrm{d}G_{\tau_N}}{\mathrm{d}x}(x) = \frac{N}{p-q} \tag{3.2.1}$$

if $p > q$. If $p \leq q$, the limit diverges and the expected hitting time is infinite, $\mathbb{E}(\tau_N) = \infty$.

3.2.2 Two Boundaries at $-N$ and N

Note once again that the definition of τ_N in (3.0.2) implies that the walk will stop if it hits $-N$.

By conditioning on the first step as in [5], we have the partial difference equation

$$\mathcal{E}(k) = 1 + p \cdot \mathcal{E}(k+1) + q \cdot \mathcal{E}(k-1)$$

with boundary conditions $\mathcal{E}(0) = \mathcal{E}(2N) = 0$, where $\mathcal{E}(k) = \mathbb{E}(\tau_k)$ for $k = 0, 1, \ldots, 2N$. Solving this recurrence (detailed in Appendix B) yields

$$\mathbb{E}(\tau_N) = \mathcal{E}(N) = \begin{cases} \dfrac{N}{p-q} \cdot \dfrac{1-(q/p)^N}{1+(q/p)^N}, & \text{if } p \neq q; \\ N^2, & \text{if } p = q. \end{cases} \tag{3.2.2}$$

4 Two-Dimensional Random Walk: Reductions for Unbounded Boundaries

We now consider a general random walk $(S_n)_n$ on $\mathbb{Z}^2$ with step probabilities p_E, p_W, p_N, p_S corresponding to steps in the East, West, North, and South directions, respectively.

While the general hitting time problem in two dimensions is complex, certain boundaries allow for exact reduction to one-dimensional problems via coordinate transformation, even in the presence of bias.

To analyze the hitting time and probability for these boundaries, we write $S_n = (X_n, Y_n)$ for all $n \in \mathbb{N}$, where X_n and Y_n are random variables that take values in $\mathbb{Z}$ with a specific restriction such that $\Delta X_n = X_{n+1} - X_n$ and $\Delta Y_n = Y_{n+1} - Y_n$ are in $\{-1, 0, 1\}$. To be more precise, $(\Delta X_n, \Delta Y_n)$ can only take values in $\{(1,0), (-1,0), (0,1), (0,-1)\}$ with probabilities p_E, p_W, p_N, and p_S, respectively. We also assume that the walk starts at the origin, $S_0 = (0,0)$.

4.1 Line Boundary ($x + y = N$)

Consider the stopping time $\tau_N = \min\{n \in \mathbb{N} : X_n + Y_n = N\}$. Let $Z_n = X_n + Y_n$. Based on the transition dynamics, the increment $\Delta Z_n = Z_{n+1} - Z_n$ takes values in $\{-1, 1\}$. Specifically, a step North $(0,1)$ or East $(1,0)$ increases Z_n by 1, while a step South $(0,-1)$ or West $(-1,0)$ decreases Z_n by 1.

Let us define the effective one-dimensional probabilities,

$$p_{\text{eff}} = \mathbb{P}(\Delta Z_n = +1) = p_E + p_N,$$
$$q_{\text{eff}} = \mathbb{P}(\Delta Z_n = -1) = p_W + p_S.$$

This projection reduces the two-dimensional problem to a standard one-dimensional random walk starting at $Z_0 = 0$ targeting the boundary N.

The hitting time distribution follows (3.1.2) with p replaced by p_{eff} and q replaced by q_{eff}. Similarly, the expected hitting time is obtained directly from (3.2.1), assuming $p_{\text{eff}} > q_{\text{eff}}$,

$$\mathbb{E}(\tau_N) = \frac{N}{p_{\text{eff}} - q_{\text{eff}}}.$$

4.2 Strip Boundary ($|x + y| = N$)

Using the same projection $Z_n = X_n + Y_n$, the strip boundary condition $|X_n + Y_n| = N$ corresponds to the two-boundary problem on the interval $[-N, N]$ for the effective one-dimensional walk.

The hitting time distribution follows (3.1.4) with p replaced by p_{eff} and q replaced by q_{eff}. Similarly, the expected hitting time is obtained directly from (3.2.2), assuming $p_{\text{eff}} > q_{\text{eff}}$.

5 Two-Dimensional Random Walk: Comparison of Expected Hitting Times for Bounded Boundaries

In previous sections, we reduced certain symmetric boundaries ($x+y = N$ and $|x+y| = N$) to one-dimensional problems. However, for general bounded domains $D \subset \mathbb{Z}^2$, such as the diamond ($|x| + |y| \leq N$), the square ($|x| \leq N, |y| \leq N$), or the circle ($x^2 + y^2 \leq N^2$), no simple reduction exists.

5.1 Expected Hitting Time and the Discrete Poisson Equation

Let $E(x, y)$ denote the expected number of steps to hit the boundary starting from (x, y). By conditioning on the first step, for any interior point $(x, y) \in \text{int}(D)$, we have

$$E(x, y) = 1 + \sum_{(x',y')\sim(x,y)} p((x, y) \to (x', y'))E(x', y'). \tag{5.1.1}$$

Rearranging the terms, we can express this in terms of a discrete operator $\mathcal{L}$, often referred to as the generator of the walk,

$$\sum_{(x',y')\sim(x,y)} p((x, y) \to (x', y'))E(x', y') - E(x, y) = -1.$$

Defining the operator $\mathcal{L}u(x, y) \coloneqq \mathbb{E}\left(u(S_{n+1}) \mid S_n = (x, y)\right) - u(x, y)$, the equation succinctly becomes

$$\begin{cases} -\mathcal{L}E(x, y) = 1, & (x, y) \in \text{int}(D); \\ E(x, y) = 0, & (x, y) \in \partial D, \end{cases} \tag{5.1.2}$$

a Poisson equation with Dirichlet boundary conditions [1, pp. 140–148].

5.1.1 Explicit Solution for $N = 2$, General (Diamond Domain)

Let us consider the diamond domain defined by $|x| + |y| \leq 2$. The interior points are $(0, 0), (1, 0), (-1, 0), (0, 1), (0, -1)$. Let p_E, p_W, p_N, and p_S be the probabilities of stepping east, west, north, and south, respectively. Then, by applying the general recurrence relation and by vanishing boundary terms, we obtain the system

$$\begin{aligned} E(0,0) &= 1 + p_E E(1,0) + p_W E(-1,0) + p_N E(0,1) + p_S E(0,-1), \\ E(1,0) &= 1 + p_W E(0,0), \\ E(-1,0) &= 1 + p_E E(0,0), \\ E(0,1) &= 1 + p_S E(0,0), \\ E(0,-1) &= 1 + p_N E(0,0). \end{aligned}$$

This gives

$$E(0, 0) = \frac{2}{1 - 2p_E p_W - 2p_N p_S}. \tag{5.1.3}$$

5.1.2 Explicit Solution for $N = 3$, Unbiased (Diamond Domain)

For the case of $N = 3$, the complexity of the system increases. The full system involves 13 interior variables. We do not present the solution for a general formula; instead, we assume the symmetry of the domain and the walk to reduce the number of unique variables to 4.

The interior points are defined by $|x| + |y| < 3$. Based on their distance from the origin and symmetry, we define the following unique variables.

- Origin: $e_0 = E(0, 0)$.
- Inner axis points: $e_1 = E(1, 0) = E(-1, 0) = E(0, 1) = E(0, -1)$.
- Outer axis points: $e_2 = E(2, 0) = E(-2, 0) = E(0, 2) = E(0, -2)$.
- Diagonal points: $e_3 = E(1, 1) = E(1, -1) = E(-1, 1) = E(-1, -1)$.

We now set up the discrete Poisson equation $4E(u) - \sum_{v\sim u} E(v) = 4$ for each unique variable.

At the origin $(0, 0)$. The neighbors are the four e_1 points; this gives

$$4e_0 - 4e_1 = 4,$$

or

$$e_0 - e_1 = 1. \tag{5.1.4}$$

At the outer axis point $(2, 0)$. The neighbors are $(1, 0)$ (value e_1) and three boundary points $(3, 0), (2, 1), (2, -1)$ where $E = 0$; this gives

$$4e_2 - (e_1 + 0 + 0 + 0) = 4,$$

or

$$e_2 = 1 + 0.25e_1. \tag{5.1.5}$$

At the diagonal point $(1, 1)$. The neighbors are $(0, 1)$ and $(1, 0)$ (both value e_1) and two boundary points $(1, 2), (2, 1)$ where $E = 0$; this gives

$$4e_3 - (e_1 + e_1 + 0 + 0) = 4,$$

or

$$e_3 = 1 + 0.5e_1. \tag{5.1.6}$$

At the inner axis point $(1, 0)$. The neighbors are the origin e_0, the outer axis point e_2, and two diagonal points e_3 (specifically $(1, 1)$ and $(1, -1)$).

$$4e_1 - (e_0 + e_2 + 2e_3) = 4. \tag{5.1.7}$$

Solving this system yields $e_0 = 39/7$.

We will see the asymptotic behavior of e_0 as N increases in 5.3.

5.2 Asymptotic Scaling and Data Collapse

A fundamental question is how the distribution $f_{\tau_N}(n)$ behaves as the domain size N increases. As in [2, p. 49], it is known that $\mathbb{E}(\tau_N) \propto N^2$. We expect that the distribution satisfies a scaling law of the form

$$f_N(n) \approx \frac{1}{N^2} \Phi\left(\frac{n}{N^2}\right), \tag{5.2.1}$$

where $\Phi(u)$ is called a universal scaling function dependent only on the domain shape, not on N. Note that the factor $1/N^2$ ensures the normalization of the probability density.

To verify this, we performed numerical simulations for square domains of varying sizes $N \in \{25, 50, 75, 100\}$. The results are presented in Figure 1.

The left panel displays the raw distributions $f_{\tau_N}(n)$, which flatten and shift to the right as N increases. The right panel shows the rescaled distributions, plotting $N^2 f_{\tau_N}(n)$ against the normalized time n/N^2.

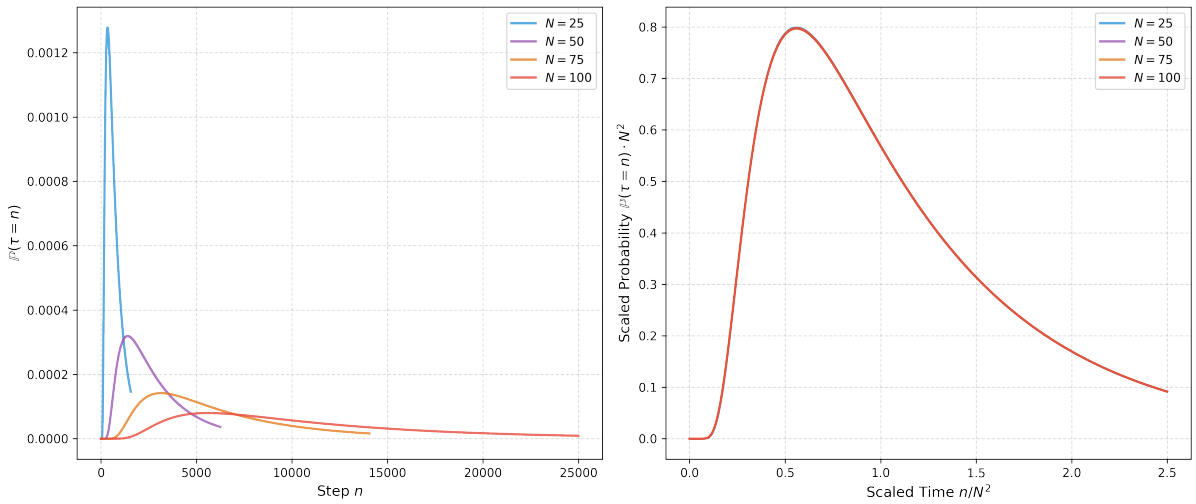

Figure 1: Asymptotic universality of the hitting time distribution. Left: Raw probability distributions for different domain sizes N. Right: Data collapse obtained by rescaling time by t/N^2 and probability by N^2, confirming our expectation.

The collapse of the curves in Figure 1 onto a single master curve is a manifestation of the functional central limit theorem (Donsker's theorem). As $N \to \infty$, the rescaled random walk converges to a planar Brownian motion [2, p. 63], which is shown in Figure 2. Consequently, the universal scaling function $\Phi(u)$ corresponds to the probability density of the first exit time of a Brownian motion from the domain $[-1, 1]^2$.

Since the components of Brownian motion are independent, this density can be expressed analytically using the spectral expansion of the heat kernel on a square [6]. The exponential tail observed in our data corresponds to the decay rate governed by the principal eigenvalue of the Laplacian on the square domain.

5.3 Numerical Comparison of Domain Geometries, Unbiased

Having derived exact solutions for small N in the diamond domain, we now extend our analysis to larger domains using numerical methods. In this section, we focus strictly on the unbiased simple symmetric random walk ($p_E = p_W = p_N = p_S = 1/4$) to isolate the effect of boundary geometry on the hitting time.

We utilized a finite difference method to solve the discrete Poisson equation defined in (5.1). We implemented a sparse linear solver to compute the expected hitting time at the origin, $E(0,0)$, for characteristic lengths N ranging from 5 to 60. We compare the diamond domain against two other standard geometries:

Diamond (L^1-ball) Defined by $|x| + |y| \leq N$. This is our primary domain of interest.

Circle (L^2-ball) Defined by $x^2 + y^2 \leq N^2$. Used as a control group due to its radial symmetry.

Square (L^∞-ball) Defined by $\max(|x|, |y|) \leq N$.

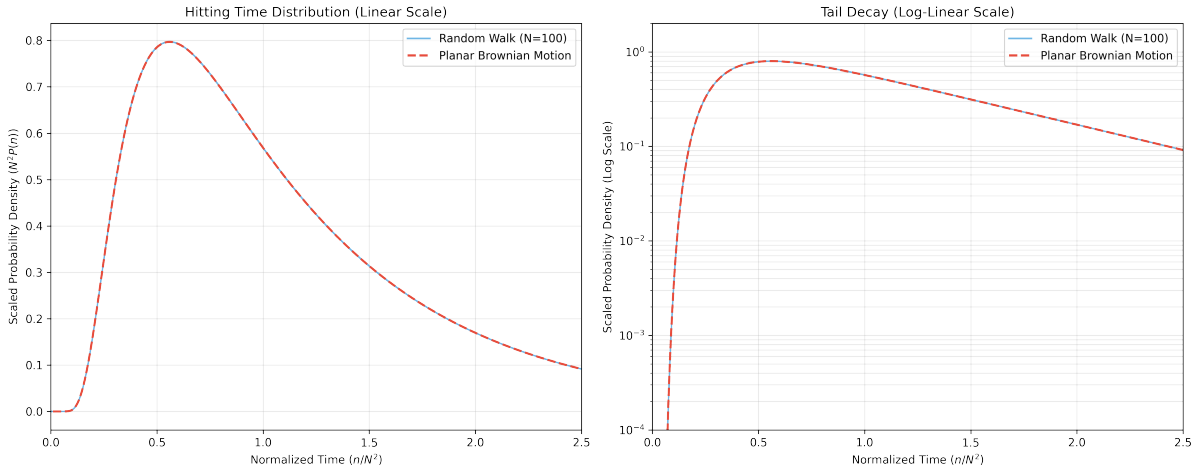

Figure 2: The comparison of hitting time distributions between random walk and planar Brownian motion. The close agreement validates the convergence of the random walk to Brownian motion in the scaling limit, confirming the applicability of continuous diffusion approximations for large domains.

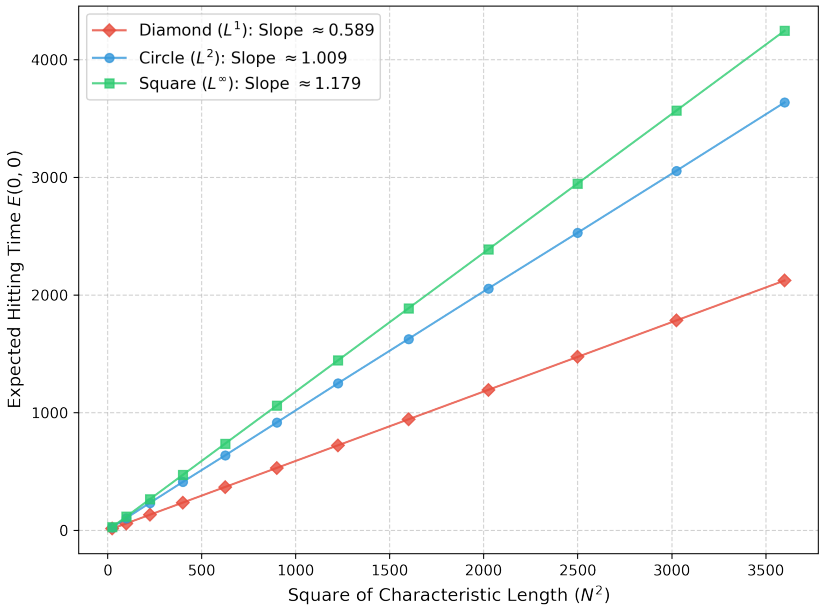

Figure 3: Comparison of the expected hitting time $E(0,0)$ scaling across three different geometries with respect to the square of the characteristic length N^2. The slopes indicate the geometric efficiency of the domain.

The numerical results are presented in Figure 3. We observe that for all three geometries, the expected hitting time scales linearly with N^2, confirming the asymptotic relationship $\mathbb{E}(\tau) = C \cdot N^2$.

The slope C represents a shape-dependent constant. Physically, the equation $-\Delta u = 4$ is analogous to the problem of finding the stress function in a beam of cross-section D under torsion. The maximum value of this stress function (our $E(0,0)$) corresponds to the peak height of Prandtl's membrane, *not* the torsional rigidity; the latter is the integral $M_t = 2\iint_D \varphi \, dA$, a quantity one power of length higher.

5.3.1 Diamond Domain (L^1-Ball)

Our numerical simulation yields a slope of $C \approx 0.589$.

To understand this constant theoretically, we recognize that the diamond $|x| + |y| \leq N$ is geometrically equivalent to a square rotated by 45° with side length $2a = \sqrt{2}N$. The expected hitting time satisfies a discrete Poisson equation, which is mathematically equivalent to the stress function in the torsion problem of a beam [7]. The connection between the random walk and the continuum torsion problem is established by matching the source terms and domain dimensions. In this study, we solve the discrete Poisson equation $-\Delta E = 4$, which corresponds to the torsional stress function φ with $G\theta = 2$. Given that the diamond domain $|x| + |y| \leq N$ is geometrically equivalent to a square with half-side length $a = N/\sqrt{2}$ and $a^2 = N^2/2$, we substitute these values into the exact infinite series solution for a square cross-section [7]. The resulting theoretical coefficient C_{diamond} is expressed as

$$C_{\text{diamond}} = 1 - \frac{32}{\pi^3} \sum_{k=0}^{\infty} \frac{(-1)^k}{(2k+1)^3 \cosh \frac{(2k+1)\pi}{2}} \approx 0.58937. \tag{5.3.1}$$

Our numerical result of 0.589 aligns perfectly with this theoretical value, confirming that the discrete random walk on a diamond lattice approaches the continuum limit of a rotated square.

5.3.2 Circular Domain (L^2-Ball)

This is used as a control group because it possesses the simplest analytical solution in the continuum limit.

In the continuum limit, the expected exit time $u(x)$ from a ball of radius R satisfies the Poisson equation $-\Delta u = 2d$ (where d is the dimension) with boundary condition $u = 0$ on $\partial B(0, R)$. According to the representation formula using Green's function [8, pp. 33–41], the solution is unique and can be expressed as an integral of the source term. Due to the radial symmetry of the domain and the operator, the solution must be a function of the radius $r = \|x\|$ only. Solving the corresponding ordinary differential equation yields

$$u(r) = R^2 - r^2. \tag{5.3.2}$$

At the origin ($r = 0$) with $R = N$, the expected time is exactly N^2. Using the fact that $\|S_n\|^2 - n$ is a martingale [2], the expected exit time is equal to the expected squared Euclidean norm at the boundary, $\mathbb{E}(\tau_N) = \mathbb{E}(\|S_{\tau_N}\|^2)$. Since the walker exits the domain slightly beyond the radius N (the overshoot is negligible for large N), the expected time is asymptotically N^2, implying $C = 1$. Our numerical simulation yields $C \approx 1.01$, which serves as a validation of our finite difference solver.

5.3.3 Square Domain (L^∞-Ball)

Our simulation yields a slope of $C \approx 1.179$.

We can explain this value directly from the result of the diamond domain without re-evaluating the infinite series.

Rotation Invariance The Laplacian operator $\Delta = \partial_{xx} + \partial_{yy}$ is invariant under rotation [8, p. 85]. Therefore, the orientation of the square (whether axis-aligned like the L^∞-ball or rotated by 45° like the L^1-ball) does not change the functional form of the solution relative to its size.

Area Scaling The area of the L^1-ball (diamond) is $2N^2$ (diagonals of length $2N$), while the area of the L^∞-ball (square) is $4N^2$ (sides of length $2N$).

Since the area of the L^∞-ball (square) is exactly twice the area of the L^1-ball (diamond), and the expected hitting time scales linearly with the area (or quadratically with the characteristic length) for the same shape, the coefficient for the square should be exactly twice that of the diamond,

$$C_{\text{square}} = 2 \cdot C_{\text{diamond}} \approx 1.17874. \tag{5.3.3}$$

This theoretical prediction matches our numerical result of 1.179 with precision. This confirms that the geometric efficiency of the domain is primarily determined by its area and shape class, while rotation plays no role in the continuum limit.

5.4 Difficulties Encountered and Solutions

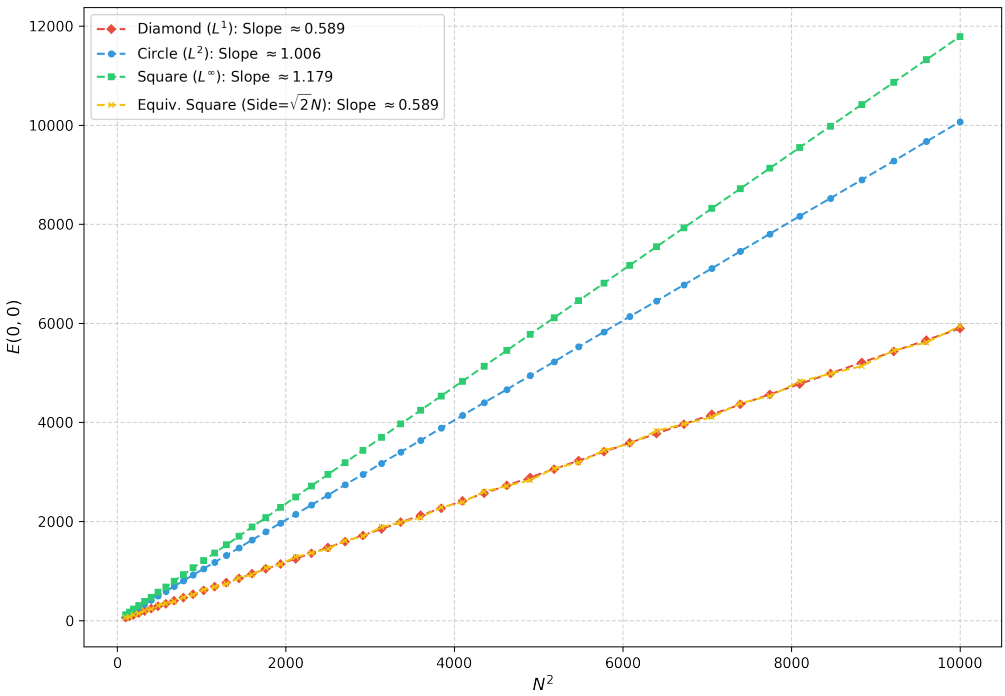

Figure 4: Scaling of the expected hitting time $E(0,0)$ for diamond, circle, square, and equivalent square geometries. The convergence of the diamond and equivalent square slopes ($C \approx 0.589$) demonstrates the rotation invariance of the underlying diffusion process.

To empirically verify that the Laplacian operator is invariant under rotation [8, p. 85], we introduced a fourth test case: a square domain oriented parallel to the coordinate axes but with a side length equal to that of the diamond domain ($s = \sqrt{2}N$). In the continuum limit, these two domains are identical up to a 45° rotation and should therefore yield the same scaling coefficient $C = C_{\text{theory}} \approx 0.58937$.

Initially, the coefficient for the equivalent square was a little off; it was $C \approx 0.592$ when using a coarse sampling interval for N. However, by increasing the sampling density (reducing the step size between successive N values from 5 to 2), the estimated slope converged to 0.589. Results are presented in Figure 4.

We observed that the values for the equivalent square exhibit subtle oscillations around the diamond's trend line. This is a discretization artifact: since the boundary must be snapped to the $\mathbb{Z}^2$ grid, the effective area of the L^∞-ball fluctuates slightly above or below the theoretical L^1-ball depending on the parity of N. Such oscillations are expected to vanish in the continuous limit.

The fact that the equivalent square and the diamond domain yield the same coefficient confirms that the expected hitting time is a fundamental geometric property. As the lattice effects are smoothed out through finer sampling, the rotation invariance of the underlying Brownian motion becomes the dominant characteristic.

This result provides strong empirical support for our earlier hypothesis that the diamond domain behaves asymptotically as a rotated square. It demonstrates that for sufficiently large N and adequate sampling, the orientation of the domain relative to the $\mathbb{Z}^2$ lattice does not alter the fundamental diffusive scaling.

5.5 Bonus: Universal Scaling in Higher Dimensions for the Circular Domain

Inspired by the consistent N^2 scaling observed in one and two dimensions (especially in 5.3.2), we extend our theoretical analysis to a general d-dimensional simple symmetric random walk on $\mathbb{Z}^d$. We consider the domain to be a d-dimensional hypersphere (ball) of radius N, defined by $\|x\| \leq N$.

Remarkably, the quadratic scaling of the expected hitting time is universal across all dimensions. This can be derived analytically by solving the corresponding Poisson equation in hyperspherical coordinates [8, pp. 33–41].

For a simple symmetric random walk in $\mathbb{Z}^d$, the expected hitting time $u(x)$ satisfies the discrete Poisson equation which converges to the continuum partial differential equation,

$$\Delta u(x) = -2d, \quad \text{for } \|x\| < N,$$

subject to the boundary condition $u(x) = 0$ on $\|x\| = N$. The source term $-2d$ arises from the variance of the step size in d dimensions (sum of unit steps in each coordinate).

Solving this partial differential equation and applying the boundary condition yields the expected hitting time as a function of the radius $r = \|x\|$,

$$u(r) = N^2 - r^2. \tag{5.5.1}$$

At the origin ($r = 0$), the expected hitting time is exactly N^2.

This derivation proves that the "curse of dimensionality" does not apply to the mean exit time from a ball; the particle escapes with the same N^2 efficiency in any dimension $d \geq 1$. This result is also consistent with the martingale property of $\|S_n\|^2 - n$ [2, pp. 263–269] which holds for any d.

6 Conclusion

This study systematically analyzed the properties of random walks, progressing from fundamental one-dimensional intervals to complex two-dimensional geometries. By incorporating drift into our analysis, we derived analytical expressions for biased walks and characterized the fundamental transition in hitting time scaling from quadratic diffusion to linear advection. Furthermore, we established that certain two-dimensional exit problems, such as those involving linear or strip boundaries, can be simplified into equivalent one-dimensional models via coordinate transformation.

The core of our investigation focused on the impact of domain geometry on hitting times in two dimensions. Through extensive numerical simulations, we demonstrated that while the quadratic scaling law $\mathbb{E}(\tau) = C \cdot N^2$ is universal for bounded domains, the specific prefactor C is strictly determined by the shape of the domain. Specifically, our results for diamond, circular, and square domains converge to constants that are perfectly predicted by continuum beam-torsion theory (specifically, the centroidal value of the stress function).

Finally, our verification of rotation invariance confirmed that the orientation of a domain relative to the lattice does not alter its asymptotic behavior, provided that discretization artifacts such as parity-dependent oscillations are properly accounted for through dense sampling. These findings bridge the gap between discrete stochastic processes and classical potential theory, providing a robust framework for predicting escape times in complex geometric environments.

Acknowledgments

I would like to express my sincere gratitude to my advisor, Prof. Yuki CHINO, for his invaluable guidance and continuous encouragement throughout this project. I am especially grateful for his support during the application process while I was on an exchange program in France. Despite the time difference, he generously made time for meetings to help me overcome challenges in writing this report. His insightful advice and clear direction have been instrumental to the completion of this research.

Appendix A: Derivation of the Expected Hitting Time for One Boundary

We work with the generating function $G_{\tau_N}(x)$ for the expected hitting time. Note that

$$G_{\tau_N}(x) = \sum_{n \geq 0} f_{\tau_N}(n) x^n,$$

where $f_{\tau_N}(n) = P(\tau_N = n)$. To find the expected value rigorously, we take the left limit of the derivative as $x \to 1^-$ by Abel's theorem, yielding

$$\begin{aligned} \lim_{x \to 1^-} \frac{\mathrm{d}G_{\tau_N}}{\mathrm{d}x}(x) &= \sum_{n \geq 1} n \cdot P(\tau_N = n) \\ &= \mathbb{E}\left(\tau_N \mathbf{1}_{\{\tau_N < \infty\}}\right) \end{aligned}$$

which represents the defective mean. This value is the true expectation $\mathbb{E}(\tau_N)$ only if $P(\tau_N < \infty) = 1$; otherwise, $\mathbb{E}(\tau_N) = \infty$ but the conditional mean $\mathbb{E}(\tau_N \mid \tau_N < \infty)$ will be finite. From the closed-form generating function, applying the chain rule gives

$$\frac{\mathrm{d}G_{\tau_N}}{\mathrm{d}x}(x) = \frac{\mathrm{d}}{\mathrm{d}x}\left(G_{\tau_1}(x)\right)^N = N\left(G_{\tau_1}(x)\right)^{N-1}\frac{\mathrm{d}G_{\tau_1}}{\mathrm{d}x}(x)$$

and taking the limit as $x \to 1^-$ results in

$$\lim_{x\to 1^-}\frac{\mathrm{d}G_{\tau_N}}{\mathrm{d}x}(x) = N\left(\lim_{x\to 1^-} G_{\tau_1}(1)\right)^{N-1}\cdot \lim_{x\to 1^-}\frac{\mathrm{d}G_{\tau_1}}{\mathrm{d}x}(x). \tag{6.0.1}$$

In (6.0.1), we must evaluate the limits of both $G_{\tau_1}(x)$ and its derivative. We first analyze $G_{\tau_1}(x)$. Recall that $p + q = 1$. Evaluating the limit of the closed-form expression for $G_{\tau_1}(x)$ as $x \to 1^-$ yields

$$\lim_{x\to 1^-} G_{\tau_1}(x) = \frac{1-\sqrt{1-4pq}}{2q} = \frac{1-|p-q|}{2q}.$$

Thus, we obtain the piecewise limit

$$\lim_{x\to 1^-} G_{\tau_1}(x) = \begin{cases} p/q, & p < q \\ 1, & p \geq q. \end{cases}$$

Next, we analyze the derivative. By the quotient rule, we have

$$\frac{\mathrm{d}G_{\tau_1}}{\mathrm{d}x}(x) = \frac{1}{(2qx)^2}\left(\frac{4pqx}{\sqrt{1-4pqx^2}}\cdot 2qx - \left(1-\sqrt{1-4pqx^2}\right)\cdot 2q\right)$$

and taking the limit as $x \to 1^-$ gives

$$\begin{aligned}
\lim_{x\to 1^-}\frac{\mathrm{d}G_{\tau_1}}{\mathrm{d}x}(x) &= \frac{1}{(2q)^2}\left(\frac{4pq}{\sqrt{1-4pq}}\cdot 2q - \left(1-\sqrt{1-4pq}\right)\cdot 2q\right) \\
&= \frac{1}{(2q)^2}\left(\frac{8pq^2}{|p-q|} - (1-|p-q|)\cdot 2q\right) \\
&= \frac{2p}{|p-q|} - \frac{1-|p-q|}{2q} \\
&= \frac{2p}{|p-q|} - \frac{p+q-|p-q|}{2q}.
\end{aligned}$$

If $p > q$, we have

$$\begin{aligned}
\lim_{x\to 1^-}\frac{\mathrm{d}G_{\tau_1}}{\mathrm{d}x}(x) &= \frac{2p}{p-q} - \frac{p+q-(p-q)}{2q} \\
&= \frac{1}{p-q}.
\end{aligned}$$

If $p = q$, the generating function simplifies to $G_{\tau_1}(x) = \dfrac{1-\sqrt{1-x^2}}{x}$. Its derivative is

$$\frac{\mathrm{d}G_{\tau_1}}{\mathrm{d}x}(x) = \frac{1}{x^2}\left(\frac{x}{\sqrt{1-x^2}}\cdot x - \left(1-\sqrt{1-x^2}\right)\cdot 1\right)$$

$$= \frac{1}{\sqrt{1-x^2}} - \frac{1-\sqrt{1-x^2}}{x^2}.$$

As $x \to 1^-$, the term $1/\sqrt{1-x^2}$ approaches infinity. Hence, when $p = q$, the limit $\lim_{x\to 1^-} \dfrac{\mathrm{d}G_{\tau_1}}{\mathrm{d}x}(x) = \infty$.

Combining these components back into (6.0.1), because $P(\tau_N < \infty) = 1$ only when $p \geq q$, the true expected hitting time diverges for $p \leq q$. We conclude that

$$\mathbb{E}(\tau_N) = \begin{cases} \infty, & p \leq q \\ \dfrac{N}{p-q}, & p > q. \end{cases}$$

Appendix B: Derivation of the Expected Hitting Time for Two Boundaries

We derive the expected hitting time $\mathbb{E}(\tau_N)$ for the random walk on $\mathbb{Z}$ with boundaries at $-N$ and N. This problem is equivalent to a random walk starting at N with absorbing barriers at 0 and $2N$. Let $k \in \{0, 1, \ldots, 2N\}$ be the position shifted by N. Define $\mathcal{E}(k)$ as the expected number of steps to hit 0 or $2N$ starting from k. Our goal is to find $\mathcal{E}(N)$. By conditioning on the first step, we have the recurrence

$$\mathcal{E}(k) = 1 + p\,\mathcal{E}(k+1) + q\,\mathcal{E}(k-1) \tag{6.0.2}$$

with boundary conditions $\mathcal{E}(0) = \mathcal{E}(2N) = 0$. Equation (6.0.2) is a second-order linear non-homogeneous difference equation.

Case 1: $p \neq q$

A particular solution to (6.0.2) is $\mathcal{E}_p(k) = \frac{k}{q-p}$. The characteristic equation for the homogeneous part is $p\lambda^2 - \lambda + q = 0$, which has roots $\lambda_1 = 1$ and $\lambda_2 = q/p$. The general solution is of the form

$$\mathcal{E}(k) = C_1 + C_2 \left(\frac{q}{p}\right)^k + \frac{k}{q-p}.$$

Using the boundary conditions,

$$\mathcal{E}(0) = C_1 + C_2 = 0,$$
$$\mathcal{E}(2N) = C_1 + C_2 \left(\frac{q}{p}\right)^{2N} + \frac{2N}{q-p} = 0,$$

we have

$$C_1 \left(1 - \left(\frac{q}{p}\right)^{2N}\right) = \frac{2N}{p-q}.$$

Thus,

$$C_1 = \frac{2N}{p-q} \frac{1}{1-(q/p)^{2N}}.$$

Substituting C_1 and C_2 back into the general solution and evaluating at $k = N$ gives

$$\mathcal{E}(N) = C_1 \left(1 - \left(\frac{q}{p}\right)^N\right) + \frac{N}{q-p}.$$

Recall that $1 - x^{2N} = (1 - x^N)(1 + x^N)$. Hence,

$$C_1(1 - (q/p)^N) = \frac{2N}{p-q}\frac{1-(q/p)^N}{1-(q/p)^{2N}} = \frac{2N}{p-q}\frac{1}{1+(q/p)^N}.$$

Therefore,

$$\begin{aligned}\mathcal{E}(N) &= \frac{2N}{p-q}\frac{1}{1+(q/p)^N} - \frac{N}{p-q} \\ &= \frac{N}{p-q}\cdot\frac{2-(1+(q/p)^N)}{1+(q/p)^N} \\ &= \frac{N}{p-q}\frac{1-(q/p)^N}{1+(q/p)^N}.\end{aligned}$$

Case 2: $p = q$

The recurrence becomes $\mathcal{E}(k) = 1 + \frac{1}{2}\mathcal{E}(k+1) + \frac{1}{2}\mathcal{E}(k-1)$. The characteristic equation has a double root $\lambda = 1$. A particular solution is $\mathcal{E}_p(k) = -k^2$. The general solution is $\mathcal{E}(k) = D_1 + D_2 k - k^2$. Boundary conditions yield

$$\begin{aligned}\mathcal{E}(0) &= D_1 = 0, \\ \mathcal{E}(2N) &= D_2(2N) - (2N)^2 = 0.\end{aligned}$$

Thus, $\mathcal{E}(k) = 2Nk - k^2$. Evaluating at $k = N$, we get

$$\mathcal{E}(N) = 2N^2 - N^2 = N^2.$$

References

[1] Frank Spitzer. *Principles of Random Walk*. 2nd ed. Springer, 1976.

[2] Gregory F. Lawler and Vlada Limic. *Random Walk: A Modern Introduction*. Cambridge: Cambridge University Press, 2010.

[3] Gordan Žitković. *Lecture 5: Random Walks - Advanced Methods*. Lecture Notes, Department of Mathematics, University of Texas at Austin. Available at https://web.ma.utexas.edu/users/gordanz/notes/advanced_random_walks_color.pdf. 2019.

[4] William Feller. *An Introduction to Probability Theory and Its Applications*. 3rd ed. Vol. 1. Equation (5.7). Wiley, 1968, p. 353.

[5] Leonid B. Koralov and Yakov G. Sinai. *Theory of Probability and Random Processes*. 2nd ed. Equation (6.15). Springer, 2007, p. 97.

[6] Horatio S. Carslaw and John C. Jaeger. *Conduction of Heat in Solids*. Oxford University Press, 1959, pp. 166–169.

[7] Stephen P. Timoshenko and J. N. Goodier. *Theory of Elasticity*. 3rd ed. Equation (g). New York: McGraw-Hill, 1970, p. 276.

[8] Lawrence C. Evans. *Partial Differential Equations*. 2nd ed. Vol. 19. Graduate Studies in Mathematics. American Mathematical Society, 2010.